

Evaluation of thermo-mechanical stress in work rolls of ring rolling mill under thermal and mechanical loading

Ali Negahban^{a,*}, Ehsan Barati^b, and Abdolali Maracy^b

^a Mechanical and Aerospace Engineering Department, Malek-Ashtar University of Technology, Shahinshahr, Esfahan, Iran

^b Malek-Ashtar University of Technology, university complex of mechanical and aerospace engineering Shahinshahr, Esfahan, Iran

ARTICLE INFO

Article history:

Received:15 January 2018

Accepted:28 February 2018

Keywords:

Ring Rolling

Thermo-Mechanical Stress

Effective thermal layer

Script Code

ABAQUS

ABSTRACT

The defect in work rolls directly influence the forming cost and the final shape of the product. The researchers tend to investigate the thermo-mechanical stress in work roll of rolling machines. These stresses may reduce the roll life. Since the investigation of the thermo-mechanical stress in work roll with real-conditions is complex, comprehensive studies by means of numerical methods are available in numerous literature. However, simulating the thermo-mechanical stress is time-consuming. So, most researchers desire to simplify the geometry and boundary conditions in order to reduce simulation cost. This paper proposes an integrated finite element model to study the thermo-mechanical behavior of work rolls during hot ring rolling process. Various methods were simulated and advantages and disadvantages of each method were discussed. Due to complexities of ring rolling process, the presented model was used in flat rolling in order to verify model integrity. After that work rolls of ring rolling mill subjected to partial boundary conditions are investigated. The results of thermal and thermo-mechanical simulations show stresses in the contact region of work rolls are rather different. However, they expressed the same results in other regions. Based on the obtained results, it is revealed that the effect of mechanical loads in the equivalent stresses should be considered and the location of equivalent maximum stress is below the surface.

1. Introduction

Hot ring rolling is an incremental forming process with coupled thermo-mechanical effect. The ring rolling process is widely used in automotive, aerospace, nuclear and other high-tech industries to produce seamless rings, such as bearing ring, gear ring, aircraft turbine ring, etc. The main advantages of ring rolling are uniform quality, smooth surface, short production time, close tolerances and a considerable saving in material and energy. Besides these advantages, favorable grain flow is the most important benefit. As the ring is being formed, the grain boundaries conform with the ring curvature providing a matrix which is highly resistant to surface cracks. This process is the preferred method of forming various rings from small diameter (Bearing's body) to very large size (Nuclear reactor's part). In order to produce a specific ring, the required force for ring rolling was 4 times less than forging [1]. The conventional process starts with preheating the billet; the billet is

then upset and pierced to prepare the preformed ring. This ring is rolled on a ring rolling mill. Figure-1 shows the main parts of radial-axial ring rolling machine. The mandrel, which is idle, moves to the main roll. The main roll is fixed and driven with a constant angular velocity. These processes cause reduction of the wall thickness, rotation of the ring and also a circumferential growth of ring to the appropriate dimension; in addition, in radial-axial ring rolling mill, both diameter and height of ring are controlled. The conical axial rolls control the height of the ring.

Since the flat rolling and the ring rolling in some cases are the same, many elementary analytical relations have been obtained from the simple processes such as sheet and flat rolling. A detailed analysis of these processes in hot conditions is more complicated. Therefore, most of the investigations explaining the process are in cold condition [2-5]. There are rarely equations for warm or hot condition showing material response with all thermo-mechanical properties.

* Corresponding author.: e-mail: Ali-negahban@ssau.ac.ir

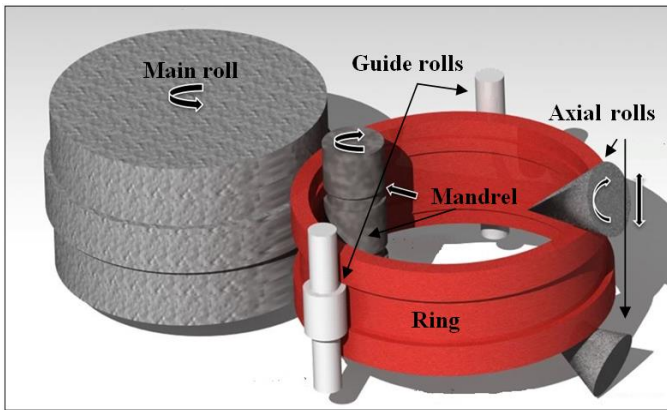


Figure 1: schematic of radial-axial ring rolling mill

Analysis of thermal stresses in the work rolls in a flat rolling machine is simple compared to ring rolling machine. Some complexity of thermo-mechanic stress analysis in ring rolling compared to flat rolling are:

- Rolling asymmetry due to the differences in the radius of the rolls (radial direction)
- Conical rolls with different diameter and velocity in contact area (axial direction)
- A roll with a rotational velocity and a roll with linear velocity and free to rotates (radial direction)
- Different contact areas because of changing the diameter of the ring within the rolling time
- Continuous increase or decrease in the thickness and height of the ring to the desired final shape
- Changing of thermo-mechanical properties and temperature during rolling time

The work rolls of a rolling process are subjected to different damages due to the contact with a hot metal such as wear, oxidation, corrosion, decarburization, etc. Considering these phenomena together make the analysis too difficult, where it is sometimes impossible to solve. It is necessary to identify the most important damages so that the analysis can be carried out based on them. Thermo-mechanical fatigue is one of these damages which is caused by non-uniform heating and mechanical loads. The thermal behavior of the work rolls in a rolling mill has always been a great interest of researchers. Inappropriate cooling may reduce the roll life due to thermal stresses. Based on simplified approximations, Steven et al. [6] reported more than 50% improvement in roll life by changing the cooling practice. To understand the influence of cooling practices on the roll life, a good assessment of the thermal stresses in a rolling process is essential [7].

With regard to above-mentioned information, investigating thermo-mechanical stress in the ring rolling is more complex than the flat or sheet rolling. Also, the boundary conditions in flat rolling are less complex than that in ring rolling.

Patula [8] developed a mathematical model to determine steady-state temperature distribution in a rotating roll subjected to constant surface heat flux over one portion and convective cooling over another portion. Yuen [9] extended Patula's solution with a strip scale layer. Tseng et al. [7] presented an analytical solution to determine the cyclic stresses produced in the roll within the rolling. Yiannopoulos et al. [10] assumed thick-walled

hollow cylinder as a work roll and investigated temperature and thermal stress distributions in rolls of metal rolling machines. Investigation of rotating functionally graded material cylinder with various boundary conditions and elastic or thermo-elastic response has been done by several researchers. Afshin et al. [11] investigated transient thermo-elastic analysis of a rotating thick cylindrical pressure vessel made of functionally graded material subjected to axisymmetric mechanical and transient thermal loads. Gharibi et al. [12] based on the Frobenius series method, studied the stresses analysis of the functionally graded rotating thick cylindrical pressure vessels. Razani et al. [13] investigated asymmetrical thermo-mechanical rolling and based on slab method and focusing on the rate-dependent flow condition, establish a new model for calculation of the rolling force. Finite element methods have successfully been used to simulate rotating cylinders with complex boundary conditions. The conditions on these cylinders are similar to the work rolls in metal forming process. However, complexities caused by several contact surfaces and many number elements in FE model makes it complicated and Time-consuming. So, many researchers often use simplifying assumptions in geometry and material properties. The temperature field of work rolls in hot and cold condition has been investigated by several authors [14-16]. Lai et al. [17] developed a general numerical method, based on a two-dimensional plane strain model, to predict the transient responses of work roll during strip rolling by coupled thermo-elasticity. Change [18] has presented a thermo-mechanical model to predict the work roll temperature distribution and the thermal stresses using a finite-difference method. Hsu et al. [19] have developed a model to estimate the surface thermal behavior of work rolls utilizing a finite-difference method. For studying the unsteady state heat transfer and the effects of various factors, Serajzadeh et al. [20] used a two-dimensional finite element method in order to predict the work roll temperature distribution during the continuous hot slab rolling process. Fischer et al. [21] investigated the temperature and the stress field in rolls of hot rolling. They presented expressions for the stress field near the surface. They indicated that it is better to use FE method for the stress field because the expressions were derived with simple assumptions. Song et al. [22], with a finite-element software program, developed a coupled thermo-mechanical model for the hot rolling of IN718 rings and predicted the surface temperature of the ring and roll. In two separate works, Benasciutti et al. [23, 24] studied the transient temperature, the thermal stress and the fatigue life of a work roll subjected to thermal loadings, which the heat flux and convective cooling rotate over roll surface. Draganis et al. [25] developed a theoretical and computational method to study thermo-mechanically coupled transient rolling contact based on an arbitrary Lagrangian–Eulerian kinematical description. Sayadi and Serajzadeh [26] used a thermal finite element analysis to determine temperature distributions within the work-piece and the work rolls and also an upper bound solution for estimating the required power in each rolling stand. Qayym et al. [27] investigated thermo-mechanical stresses in hot rolling process. Thermal and mechanical stresses produced in the work rolls during the hot rolling process are predicted by using the ABAQUS standard software. Milenin et al. [28] investigated the residual stresses in hot-rolled strips by using a numerical modeling and experimental identification. Koohbor [29] developed an integrated mathematical model to study the thermo-mechanical behavior of strips and work rolls during the warm rolling process of steels. The model was first employed to solve the thermo-mechanical response of the rolled strip under steady-state conditions and then used to apply proper boundary conditions for solving the thermo-mechanical response of the

work roll. Benasciutti et al. [30] used an 1D harmonic element which permits the analysis of plane axisymmetric structures subjected to non-axisymmetric loads and save the computational time. Deng et al. [31] investigated the microstructure, temperature, and thermal stress evolution in a high-speed steel work roll under service conditions during the early stage of hot rolling. They concluded that the residual stress at work roll surface was compressive.

According to preceding paragraphs, the most researches on thermo-mechanical stress in the rolling process are devoted to flat rolling. There are a few numerical works in thermo-mechanical assessment of the ring rolling process. In summary, the main difference between the present activity and the mentioned works are variable contact area, force and, heat flux during the simulation. Using the developed code in ABAQUS, the time-dependent mechanical and thermal loads apply to model, simultaneously. Also, this code is able to save time and maximize the accuracy.

Modeling concentrated forced convection in conventional finite element package (such as ABAQUS, ANSYS, and etc.) in the graphical user interface is not introduced. This type of modeling requires developing a code. So, three types of modeling are proposed and the results were compared. Advantages and Disadvantages of each modeling were discussed. With respect to above comparisons in this research, a 2D modeling of work rolls in ring rolling process has been introduced to evaluate thermo-mechanical stress. The prepared code has less computational cost and also able to use in any geometry with various boundary conditions.

2. Finite element modeling

Transient heat transfer in a three-dimensional anisotropic solid (Ω) bounded by a surface (Γ) is governed by the energy equation-1:

$$\left(\frac{\partial q_x}{\partial x} + \frac{\partial q_y}{\partial y} + \frac{\partial q_z}{\partial z} \right) + Q = \rho c \frac{\partial T}{\partial t} \tag{1}$$

Using finite element formulation, the solution domain (Ω) is divided into M elements with r nodes. By carrying out some mathematical procedures, equation-1 be converted to following equation for nonlinear transient heat transfer problem. Nonlinearities arise from temperature dependent properties, radiation heat transfer, and temperature dependent heat flux.

$$\begin{aligned} [C(T)]\{\dot{T}\} + [[K_c(T)] + [K_h(T, t)]]\{T(t)\} = \\ \{R_Q(T, t)\} + \{R_q(T, t)\} + \{R_h(T, t)\} + \\ \{R_\sigma(T, t)\} + \{R_r(T, t)\} \end{aligned} \tag{2}$$

In equation-2, C is element capacitance matrix, K_c and K_h are element conduction and convection matrices, the vectors R_Q , R_q , R_h are heat load vectors due to internal heat generation, specific surface heating, and surface convection, respectively. R_σ and R_r arise from surface radiation. The equation indicates that elements matrices and heat load vectors are both temperature and time-dependent. So, a solution by time marching scheme is required [32].

The equations of linear thermo-elasticity could be obtained from kinematic relation, equations of motion, energy-scale equation, and constitutive equations. The resulting thermo-elasticity equations in tensor notation are as follow[33]:

$$(C_{ijkl}\epsilon_{kl})_{,j} + (\beta_{ij}\theta)_{,j} + \rho F_i - \rho \ddot{u}_i = 0 \tag{3}$$

$$(k_{ij}\theta_{,j})_{,i} - \rho c \dot{\theta} + \rho R + T_0 \beta_{ij} \dot{\epsilon}_{ij} = 0 \tag{4}$$

C_{ijkl} , ϵ_{kl} , β_{ij} , k_{ij} , F_i , R , T_0 , u_i , θ are elasticity tensor, linear strain tensor, thermo-elasticity tensor, thermal conductivity tensor, external force per unit mass, strength of the internal heat source per unit mass, initial temperature, displacement vector, and temperature difference, respectively. $()_{,i}$ indicates partial differentiation with respect to coordinate (i). The finite element formulation of the problem is obtained in the standard way. The resulting equation expressed by matrices is shown in equation-5: [17]

$$\sum_{e=1}^N \left\{ \begin{aligned} & \left[\begin{array}{cc} [M^{(e)}] & 0 \\ 0 & 0 \end{array} \right] \left\{ \begin{array}{l} \{\ddot{u}^{(e)}\} \\ \{\ddot{\theta}^{(e)}\} \end{array} \right\} + \\ & \left[\begin{array}{cc} 0 & 0 \\ [H^{(e)}] & [C^{(e)}] \end{array} \right] \left\{ \begin{array}{l} \{\dot{u}^{(e)}\} \\ \{\dot{\theta}^{(e)}\} \end{array} \right\} + \\ & \left[\begin{array}{cc} [K_1^{(e)}] & [G^{(e)}] \\ 0 & [K_2^{(e)}] \end{array} \right] \left\{ \begin{array}{l} \{u^{(e)}\} \\ \{\theta^{(e)}\} \end{array} \right\} \end{aligned} \right\} = \left\{ \begin{array}{l} \{F_1^{(e)}\} \\ \{F_2^{(e)}\} \end{array} \right\} \tag{5}$$

The general form of the equation could be as follow:

$$Ma + Cv + Kd = F \tag{6}$$

In equation-6, M, C, K, a, v, d, and F are the generalized mass, damping and stiffness matrices, generalized acceleration, velocity, displacement and external force vectors, respectively. With respect to equation-6, if the speed and acceleration of the elements are ignored, some terms in matrices will be ignored and the amount of computing time will be reduced. So, one of the strategies is to rotate the boundary condition around the roll and the roll be fixed. This assumption reduces the effective matrices in the finite element model.

ABAQUS software has the Film and the D-flux subroutines for thermal analysis. These subroutines can be used to define a non-uniform film coefficient or heat flux as a function of position, time, temperature, etc. in a heat transfer analysis [34]. Therefore, thermo-mechanical analysis needs another time-consuming simulation to convert this temperature field history to stress field [24]. In order to conquer this problem and save time, other possible methods have been investigated in this paper.

The first model, simulated by the first method, has two additional parts which are attached to the work roll as depicted in Figure-2(b). All degrees of freedom of these parts are fixed. These parts are used to facilitate modeling of concentrated convection and heat flux in the simulation. Since these parts are not in real condition, their thermo-mechanical properties should be selected carefully. In order to transfer heat flux rapidly through these parts, higher conductivity and lower heat capacity are preferred. However, there are some limitations in material properties which will be expressed later. As the roll rotates, the partial boundary conditions are applied to these parts. The angles α , γ , β are the angle of heating zone, the angle of cooling zone and the angle between two zones, respectively.

The second and third models are prepared by developing a script python code. Without attached parts, these codes were developed in ABAQUS Python Development Environment. The explicit and implicit algorithms are used in the second and third models, respectively. According to simulation requirements, these models contain several sub-models, in which boundary conditions are changed. In these models, the cooling and heating zones are rotated in reversed direction by the script code. In every step, the surface elements located on this zone are selected. Figure-2 shows these models.

Figure-3 shows an algorithm used in the second and third models. The algorithm is explained briefly as follow:

1. The desired data are collected and the desired precision is determined. This phase has a direct influence on duration of simulation and accuracy of results. Although a greater precision leads to a higher accuracy, it also causes more processing time.
2. The model is produced by script code. The ABAQUS scripting interface allows users to bypass ABAQUS graphical user interface (GUI) and communicate directly with the kernel. The sub-models create and modify during simulation.
3. The variable initial and boundary conditions are imposed on the roll in the desired steps. In each step, the boundary conditions such as rolling force, the area of heating and cooling zones, etc. are changed. To simulate the rotation of the roll, the partial boundary conditions are rotated in reverse direction. It should be noted that in each step a simple thermo-mechanical stress analysis is solved.
4. The problem is solved in a pre-selected period of time.
5. The results are extracted and used as an initial state condition for the subsequent sub-model.
6. The process will be continued until the simulation is completed.

3. Analysis of flat rolling

In most applications of explicit analysis, the mechanical response will control the stability limit. The thermal response may govern the stability limit when the material properties are

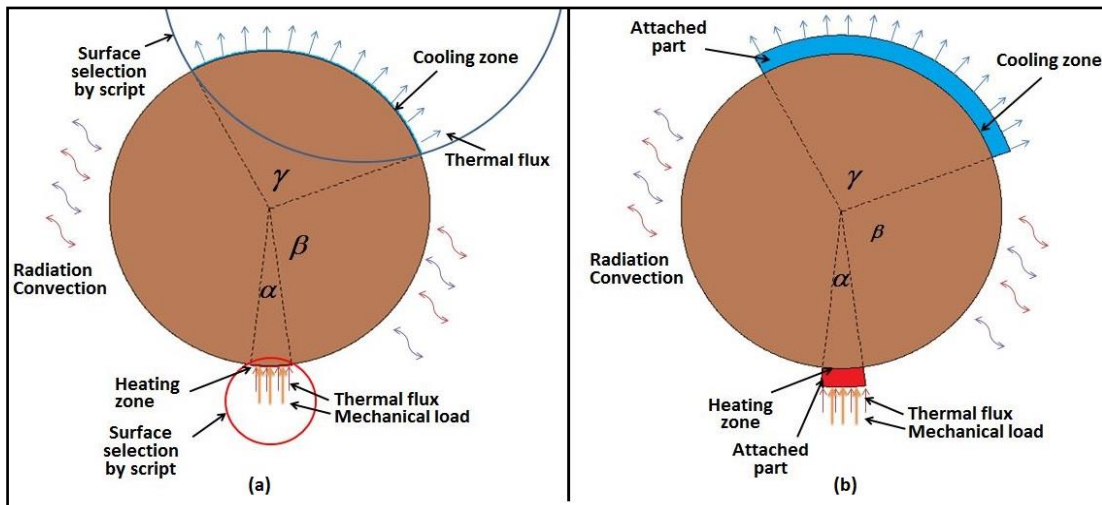


Figure 2: Work roll modeling with a partial boundary condition- (a) Surfaces selection by scripting code- (b) Attached parts

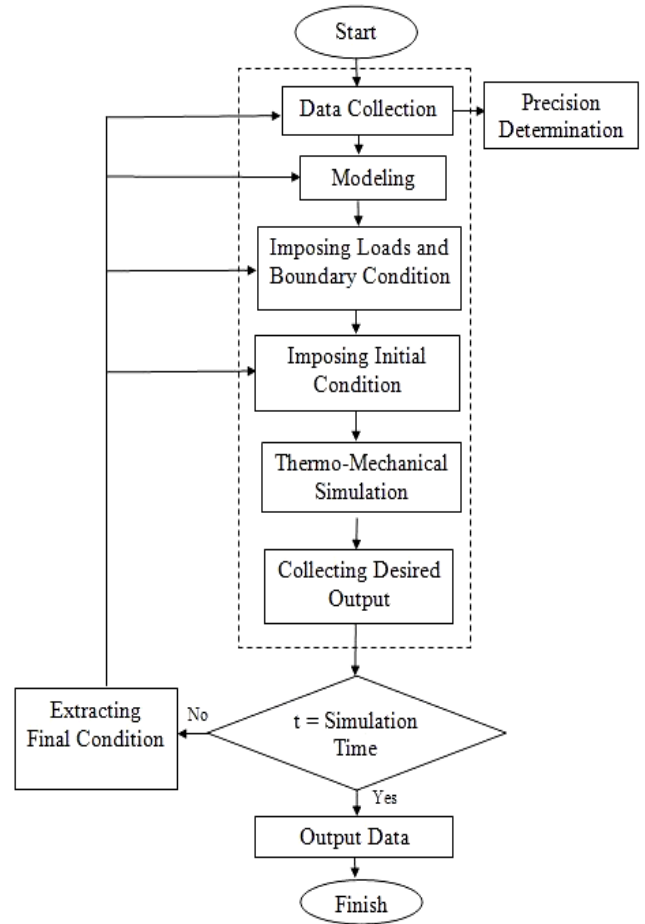


Figure3: flow chart used in first and second models

non-physical. An approximation of the stability limit for the forward-difference operator in the thermal solution response is given in equation-7[34]:

$$\Delta t \approx \frac{L_{\min}^2}{2\alpha} \quad (7)$$

Where L is the smallest element dimension in the mesh and α is the thermal diffusivity of the material calculated by the

following equation:

$$\alpha = \frac{k}{\rho c} \quad (8)$$

The parameters k , ρ , and c represent the material's thermal conductivity, density, and specific heat, respectively. Equation 7 describes the limitation that was discussed in the first model: higher conductivity and lower heat capacity facilitate movement of heat flux through the attached parts and reduce the stability limit. As a result, for avoiding divergence and obtaining a correct result, the suitable values for k , ρ , and c must be selected by trial and error in the first model.

In ABAQUS /Standard, temperatures are integrated using a backward-difference scheme, and the nonlinear coupled system is solved using Newton's numerical method. ABAQUS offers both an exact and an approximate implementation of Newton's method for fully coupled temperature-displacement analysis.

In ABAQUS /Explicit heat transfer equations are integrated using the explicit forward-difference time integration rule. The mechanical solution response is obtained using the explicit central-difference integration rule with a lumped mass matrix. Heat transfer and mechanical solutions are obtained simultaneously by an explicit coupling. The explicit integration may decrease computation time and simplify the treatment of contact.

The explicit algorithm is conditionally stable, despite the implicit algorithm. However, both algorithms need their respective specific time increment limit for avoiding divergence or spurious oscillations[32].

The research conducted by Benasciutti [30] was used to compare the temperature field in the models. The roll FE model has a fine mesh (Figure-4), with a total of 10800 elements and 11161 nodes. The outer surface is divided into 360 segments. The radial partitions are divided by seed 30 and bias 15. The first model has two contact surfaces. So in order to decrease the processing time, explicit algorithm and four nodes linear element

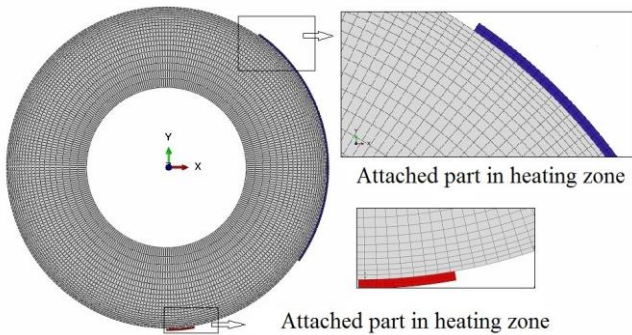


Figure4: Finite elements model of a work roll with attached parts (CPE4RT) is used. The other models use the same mesh.

The results are obtained from the models and are shown in figure-5. Variation of the node temperature ($T(^{\circ}C)$) in the surface of the roll within the period 2~4(s) is shown in this figure. The same temperature trend has been predicted by the models. In other words, the surface temperature rises rapidly in the heating zone. When roll surface leaves this zone, surface temperature decreases with a specific trend. In cooling zone, the surface temperature decreases rapidly so, there is a cusp at the point

where the cooling zone is started. When the roll leaves this zone, the surface temperature rises slowly. This is due to heat transfer from the internal nodes to external nodes.

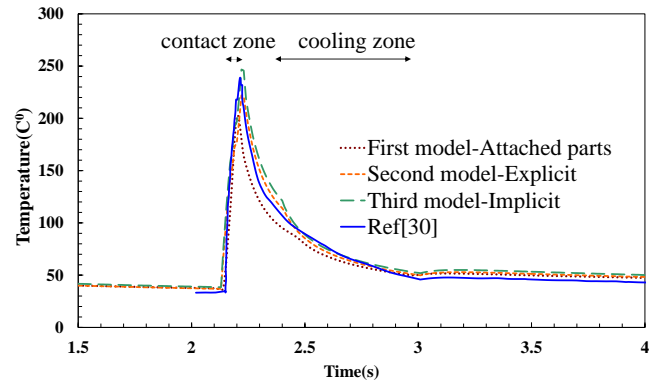


Figure5: Variation of surface temperature in different models

In the heating zone where the pick point occurred, the third model (implicit algorithm) predicted the temperature a little more than the Benasciutti's results and second model (explicit algorithm) have been predicted the temperature lower than those. In other locations, the predicted temperature, in general, is higher. The first model gives the lower temperature in this period. By using several simulations in the first model, it can be concluded that it is better to use experimental results as well as trial and error data to evaluate correct values of the virtual thermo-mechanical properties. The most advantage of first modeling method is simplicity.

The temperature of five nodes in the different depth of the third model is shown in figure 6. In the nodes closer to work roll's surface, the temperature variations are significant. The abrupt change in the temperature field was seen on and near the surface of the roll within the rolling time period. In general, all node temperatures tend to increase in spite of the roll's cooling. Also, the figure depicts the surface temperature in specific time period become lower than beneath surfaces. This phenomenon may lead to tensile stress in roll surface. Since this tensile stress may reduce roll life, there is an optimum amount of surface cooling to reduce tensile stresses in work roll. It should be noted that when there is not a sudden change in the boundary condition, all models present the same results.

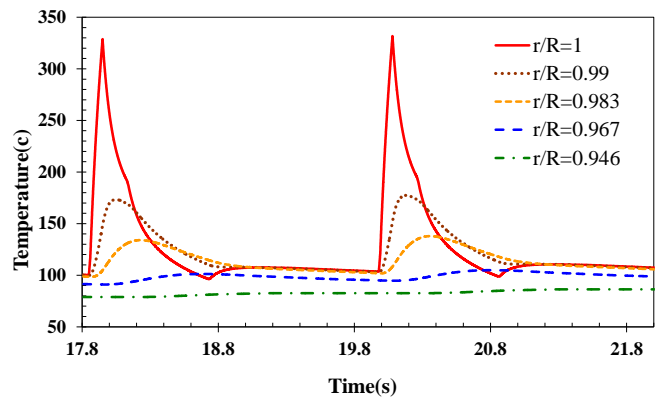


Figure6: Temperature time histories for nodes at different radial depth in normalized radial coordinate r/R .

Comparison between models which prepared by script code indicated that simulation time is almost the same. The simulation time with the personal computer (Core i7 4790-3.5GHz, RAM-

16G) took about 10 hours. This thermo-mechanical simulation by Benasciutti took 13 days [24] and in other work with a 1D parametric element, which allows the analysis of plane axisymmetric structures, it required 5 hours[30].

The advantage of this modeling procedure compared with the Benasciutti work is the ability to simulate 2D and 3D geometry without any simplification and also simulate thermal and mechanical analyses simultaneously¹. The other advantages are the ability to impose the mechanical load history and variable contact surfaces into a model.

With regard to preceding paragraph, in order to impose the concentrated forced convection and partial boundary conditions on work roll, the python code is more acceptable. If several contact surfaces are used the explicit algorithm is superior to the implicit algorithm. Otherwise, the implicit model is better due to larger stable time increment.

4. Modeling of work rolls in ring rolling mill

Precise Analysis of the ring rolling needs a 3D modeling. Although in some cases, investigators prefer to use 2D modeling to reduce the complexity of the process. The authors investigated the 3D ring rolling process in the cylindrical work rolls and ring. The 3D analyses take several days or months according to simulation time (stable time increments in the simulation was about 10^{-10} - 10^{-12}). Negahban et al. [35] investigated the 2D simulations in the ring rolling in the finishing step. It was found that when the mandrel velocity, the feed amount[36], and deformations are small, 2D and 3D models give almost same results. Also, the effect of heat generations due to deformation and friction in the temperature field was investigated. It was determined that de-coupling the ring and rolls interactions are acceptable.

In this paper, the thermal and thermo-mechanical stresses are investigated in the main roll and mandrel of rolling mill. Since contact surfaces are omitted in the simulations, using the implicit algorithm is acceptable. The Thermal and mechanical load in every step are imposed to the roll. The variation of heat flux due to ring's temperature is included in the simulation. Song et al. [22] studied hot ring rolling and used experimental data for ring's temperature in their paper. This data are used and linearized. This fitted curve is used in the simulation. The geometrical, thermal, and mechanical parameters of work rolls are listed in table-1. The properties are extracted from references [37-39] and, if necessary, the fitted curve on these data is extracted. The mechanical load and thermal heat flux are applied to surface that is located in the heating zone with a specific length. The length of these surfaces (C_1 , C_2) is obtained by equations proposed by Forouzan et al.[40]. The C_1 , C_2 are the contact lengths of the ring with the main roll and mandrel. The values of C_1 and C_2 in the first and final steps of the rolling process are obtained. A linear curve is fitted to these points and used in the developed code.

For applying the load to the analyses, the results of previous research [35] is used. The load history is shown in figure-7. The results are obtained from dynamic simulation of the ring rolling. The magnitude of pressure is computed by the load and contact

area in specific time. It should be noted that the contact surfaces and loads are changed at each simulation step.

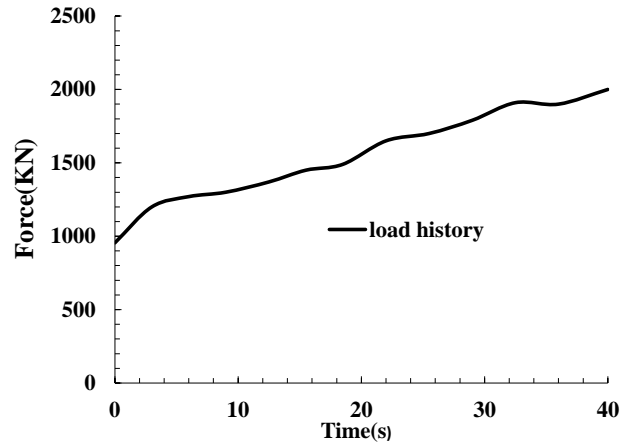


Figure7: Load history for applying the contact pressure to work rolls

5. Results and discussion

The hot ring rolling simulation is performed with the novel method to evaluate the temperature and stress fields. As mentioned before, the simulation has several steps, in which, the boundary conditions are changed. For evaluating thermo-mechanical stress analysis in ring rolling, the script code is used.

Figure-8 shows temperature time histories for nodes at different radial depth in the main roll and mandrel. Figure-8 covers the time between 0 and 6 seconds. This figure indicates that the temperature of the work rolls increases. Accordingly, it can be inferred that only the outer layer of the roll with the specific thickness experiences considerable temperature changes. The thickness of this layer can be measured by equation-9 presented by Tseng et al. [41]. The δ is the thermal boundary layer and can be expressed as the normalized distance from the roll surface ($\frac{r}{R} = 1 - \delta$). In this layer, the temperature difference between the local value and the core temperature reaches 1% of the core temperature.

$$\delta = \frac{2}{\sqrt{2Pe-1}} \ln \left[\frac{200Bi(\sqrt{2Bi}/\sqrt{Pe+2})}{\theta_0 \sqrt{Pe/2}(Bi^2/Pe + \sqrt{2Bi}/\sqrt{Pe+1})} \right] \quad (9)$$

In this equation Pe and Bi are the Peclet and Biot numbers, respectively. These numbers calculated as follow:

$$Pe = \omega R^2 / \alpha_r \quad (10)$$

$$Bi = h_0 R / k_r \quad (11)$$

Where ω is the angular velocity of the roll, R is the roll radius and α_r is the thermal diffusivity, h_0 is a uniform convective cooling, k_r is the thermal conductivity and θ_0 is the bite angle. Tesng et al. [42] have suggested that in case the convection coefficient is variable, the maximum value should be applied. With respect to data listed in table 1 and using the relation 9, the thickness of thermal layer in the main roll is 0.056. This value in the mandrel is 0.097. The computed thicknesses indicate that more than 94% of the main roll and 90% of the mandrel are uniformly at the core temperature. However, figure 8 shows that severe alterations in temperature occur in a thinner layer when compared to the analytical results.

¹ -In ABAQUS user guide manual mentioned, when contact conditions exist and the heat conducted between surfaces may depend on the separation of the surfaces or the pressure transmitted across the surfaces, the thermal and mechanical solutions should be obtained simultaneously rather than sequentially

The thinner layer which is simulated by FE software is the effective thermal layer in the transient situation. In this layer, variation of the temperature and thermal stress is noticeable. The thickness of effective thermal layer with respect to simulation results shows that the Tseng et al. relation is upper bound for this layer. Figure 8 also shows that the temperature variation of the mandrel in the effective thermal layer and its depth is more than that of the main roll which is consistent with the computed one. In the mandrel, the heat flux penetrates rapidly because of its higher speed and contact surface compared to the main roll.

Figure 9 shows the variations of Von-Mises stress and temperature of the surface element located at angular position -100° (deg) in the time period between 8-10 seconds. As expected, the maximum temperature in the work rolls increases the equivalent Von-Mises stress. In addition, the Von-Mises stress has a similar trend to that of temperature variations. The high temperature gradient causes rapid temperature changing at the thermal boundary layer of the work roll. This phenomenon causes higher thermal stresses in the layer. The figure also indicates thermo-mechanical stress with and without mechanical loads in the contact surface. It is observed that the mechanical loads mainly affect the stress distribution in the contact region. The mechanical loads have the insignificant effect on the thermo-mechanical stresses developed within the work rolls in other regions. In this time period, the magnitude of stress in contact zone with imposing load reaches 297MPa and without imposing load reaches 147MPa. The magnitudes of the thermal and thermo-mechanical stresses in other location have the same value, generally.

Figure-9(b) shows the detailed view and difference between the magnitude of thermo-mechanical stress in the element centroid and integration point, as well. In contact zone, the magnitude of thermo-mechanical stress in the integration point is 30% more than element centroid. However, in other zones, the difference between these values is insignificant. In the stress analysis, the stress values at the integration points are more accurate than other points [43].

Figure 10 shows thermal and thermo-mechanical stresses in a cylindrical coordinate. Figures 10-a and 10-c indicate stress along θ -direction within the specific time period (4-6s). The hoop stresses in various depth of the roll are compressive which are consistent with some works [31, 44]. These figures indicate the effect of mechanical loads at the heating zone. In the contact region, the hoop stress related to thermal load reaches -133MPa, whereas, the hoop stress related to thermal and mechanical load reaches -678MPa. In this zone, the thermo-mechanical stress is 5 times more than thermal stress. In the cooling zone, the magnitude of the surface hoop stress become lower than the beneath surfaces in a thin layer. If the outer surface becomes much cooler than the beneath surfaces, it may lead to tensile stress. As mentioned before, in other regions, the difference between the thermal and thermo-mechanical hoop stresses are insignificant. Figures 10-b and 10-d show the stress along r-

direction within the specific time. It is obvious that the radial stress without mechanical load is negligible. Also, the magnitude of the radial stress with imposing load is approximately equal to the hoop stress and has a significant effect on the equivalent stress. The magnitude of the radial stress before the contact zone reaches 66MPa and then, in contact zone, this value reaches -619MPa.

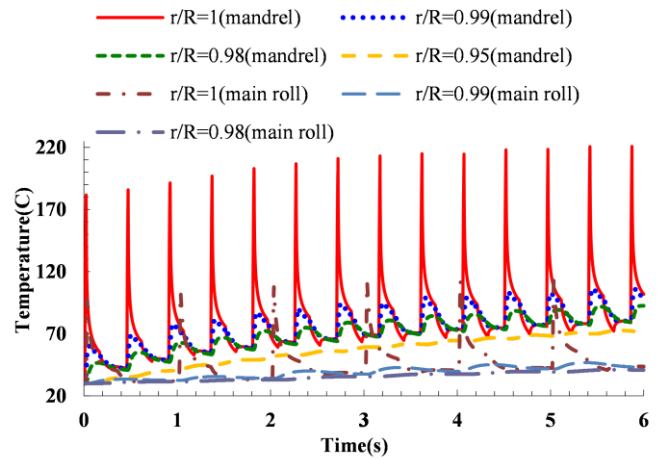


Figure 8: Temperature time histories of work rolls at different radial depth

Figure 11 shows thermal and thermo-mechanical stresses at the end of the rolling process. As expected, figures 10 and 11 show that the hoop stress is increased. The thermal and thermo-mechanical hoop stresses reach to -144MPa and -874MPa, respectively. During the process, all nodal temperatures are increased. In the cooling region, when the surface temperature becomes lower than beneath surface, the magnitude of hoop stress becomes lower than surface stress. This phenomenon is clearly seen in figure 10-a and 11-a. Figure 11-b and 11-d show the radial stress by the end of process. In the model without mechanical load, the magnitude of radial stress decreases because of reduction in temperature gradient in thermal layer. However, with imposing the load, the magnitude of the thermo-mechanical radial stress reaches -814MPa which is much more than thermal stress. Before contact zone, this value reaches 87 MPa. The reason for this can be explained as follows. The cylindrical stress components have been computed from the Cartesian component. Generally, stresses in the finite element method are manipulated by nodal displacements. As the nodal surface of an element reach to an area near the contact region, the distance between the nodes increases rapidly because of high pressure on the front node. According to the description, the magnitude of tensile stress in y-direction rise rapidly compared with other stress components. So, the computed radial stress becomes tension in this zone. However, the thermal expansion in heating zone neutralizes the effect of pressure load. So, this tensile stress vanishes when the work roll leaves the heating zone.

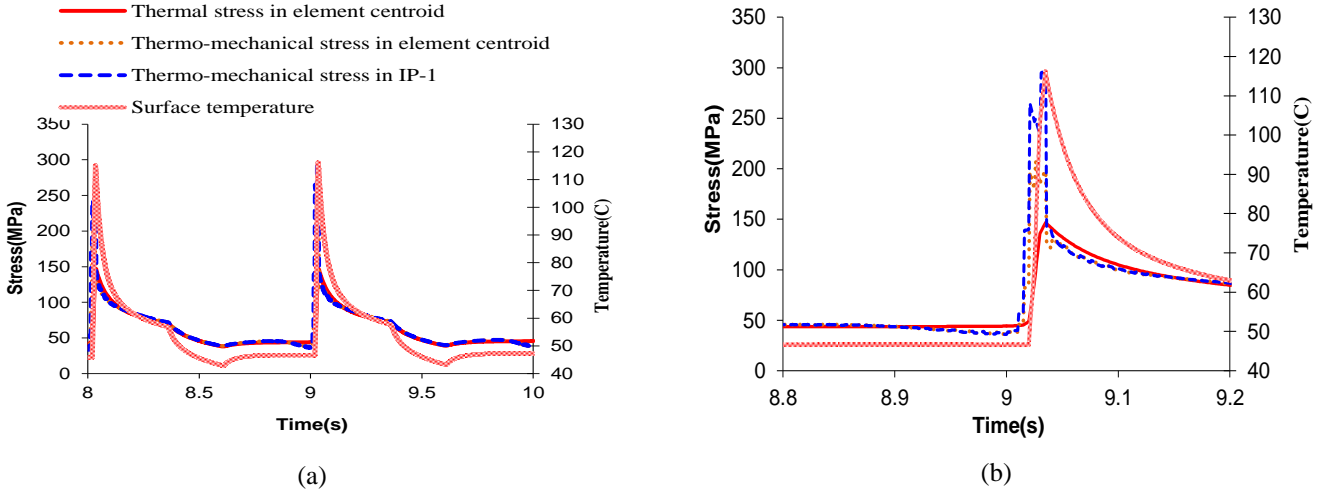


Figure 9: (a)-Variation of surface Von-Mises stress and temperature in main roll with and without imposing load-(b) Detailed view

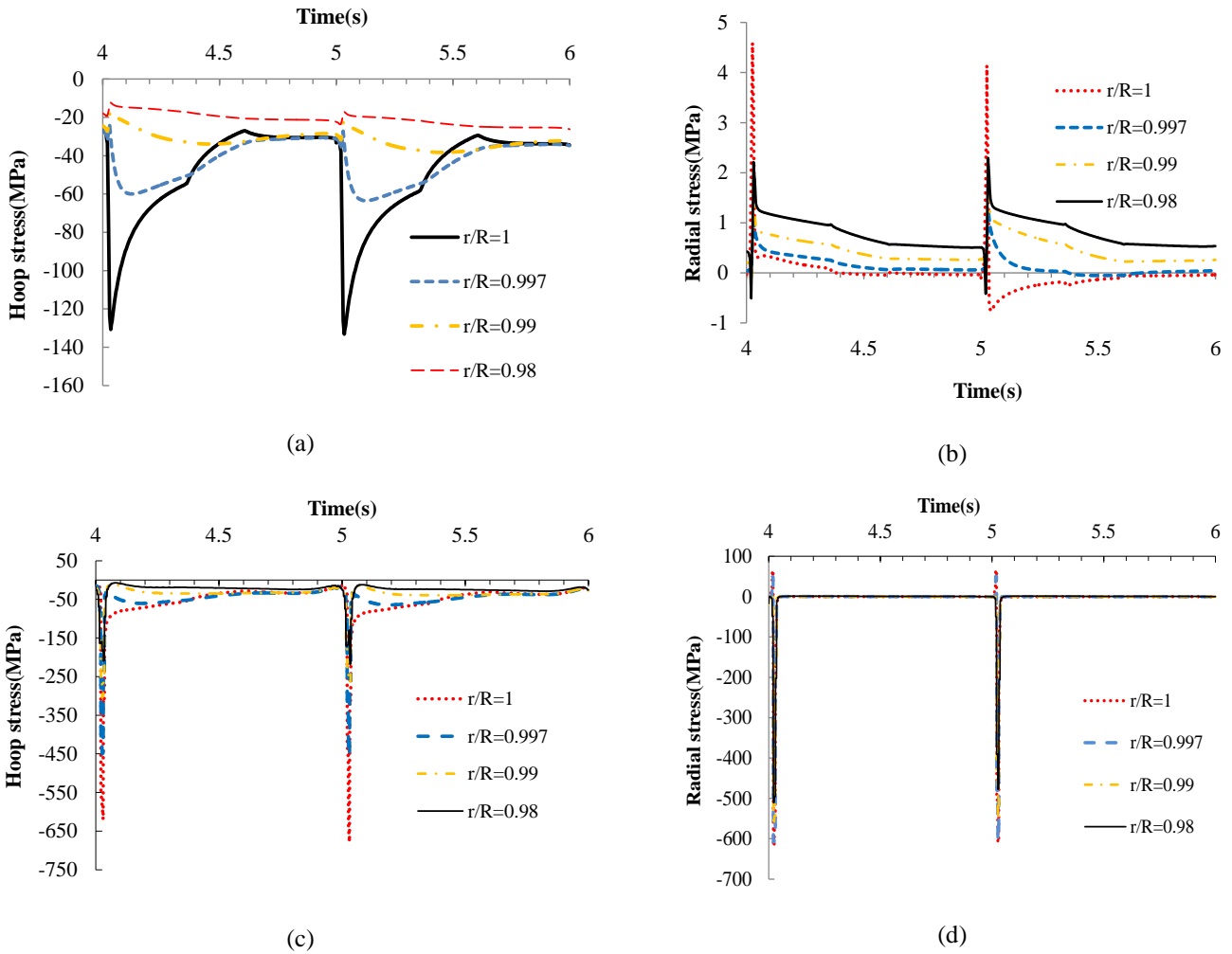


Figure 10: Variation of radial and hoop thermo-mechanical and thermal stresses in the main roll with and without imposing load within time period 4-6(s). (a) and (b) thermal stresses. (c) and (d) thermo-mechanical stresses.

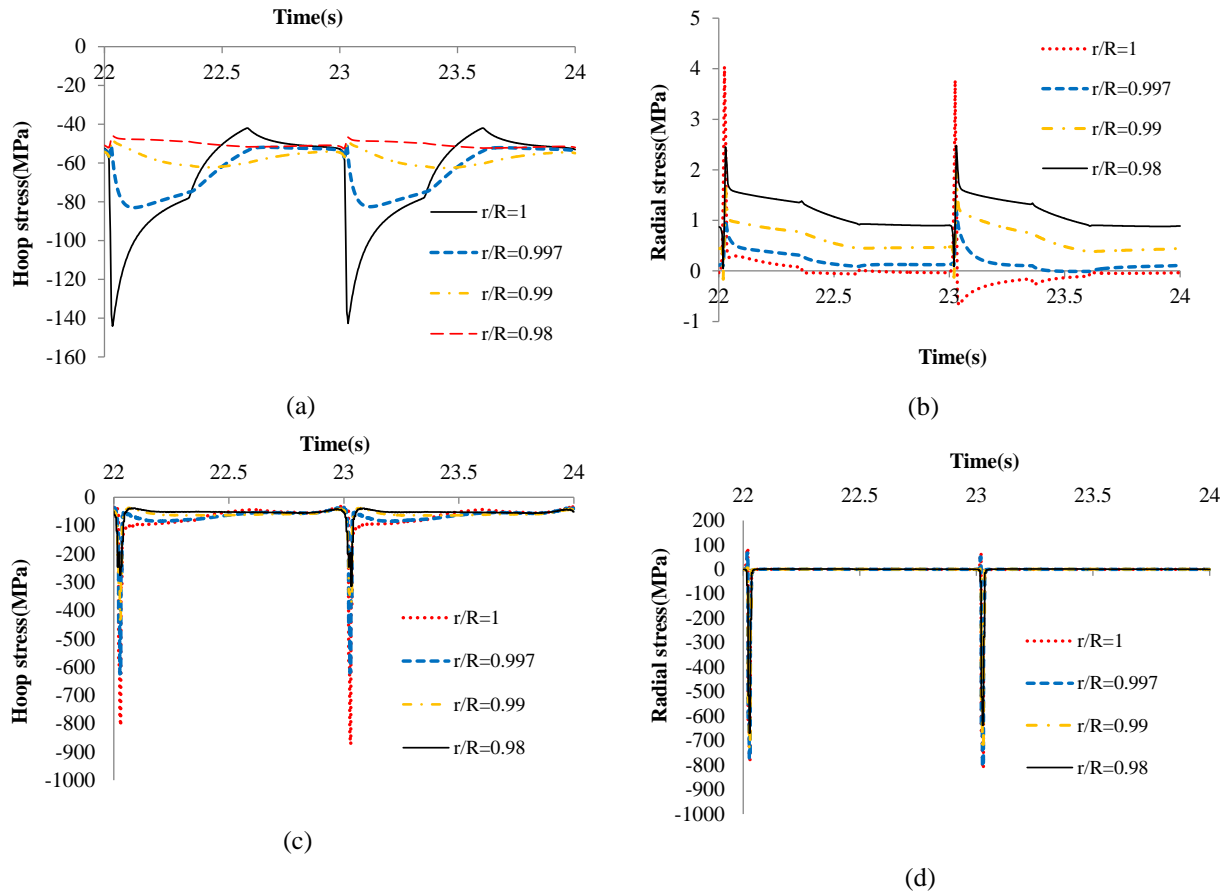


Figure 11: Variation of radial and hoop thermo-mechanical and thermal stresses in the main roll with and without imposing load within time period 22-24(s). (a) and (b) thermal stresses. (c) and (d) thermo-mechanical stresses.

Table 1: Geometrical, Thermal and mechanical properties of work rolls

Work rolls material	H-13 tool steel	Ring temperature as a function of time ($^{\circ}C$)	$1050 - 5.85t$
Radius of mandrel (mm)	60	Specific heat ($J / (kg \cdot ^{\circ}C)$)	460
Radius of main roll (mm)	200	Density (kg / m^3)	7840
Height of rolls (mm)	200	Poisson coefficient	0.285
Length of contact area on main roll (mm)	$C_1 = 7.45 + 25 \cdot 10^{-3} \cdot t$	Environment and coolant temperature ($^{\circ}C$)	30
Length of contact area on mandrel (mm)	$C_2 = 10.63 - 6 \cdot 10^{-2} \cdot t$	Forced convection coefficient ($W / (m^2 \cdot ^{\circ}C)$)	10100
Angular velocity of main roll (rad / s)	6.28	Environment convection coefficient ($W / (m^2 \cdot ^{\circ}C)$)	50
Angular velocity of mandrel (rad / s)	13.95	Contact heat conductivity ($W / (m^2 \cdot ^{\circ}C)$)	10000
Cooling sector (deg)	90	Specific heat ($J / (kg \cdot ^{\circ}C)$)	460
Angular gap between heating and cooling (deg)	120	Initial rolls temperature ($^{\circ}C$)	30
Elastic module (GPa)	186		
Flow stress as a function of plastic strain (MPa)		$\sigma_p = -268.72 \cdot \varepsilon_p^6 + 1795.5 \cdot \varepsilon_p^5 - 4676.9 \cdot \varepsilon_p^4 + 5995 \cdot \varepsilon_p^3 - 3943.2 \cdot \varepsilon_p^2 + 1334.7 \cdot \varepsilon_p + 693.05$	
Thermal conductivity as a function of temperature ($W / (m \cdot ^{\circ}C)$)		$k = 10^{-7} \cdot T^3 - 10^{-4} \cdot T^2 + 5.78 \cdot 10^{-2} \cdot T + 16.131$	
Thermal expansion as a function of temperature ($10^{-5} / ^{\circ}C$)		$\alpha = 3 \cdot 10^{-7} \cdot T^2 - 10^{-4} \cdot T + 1.0971$	

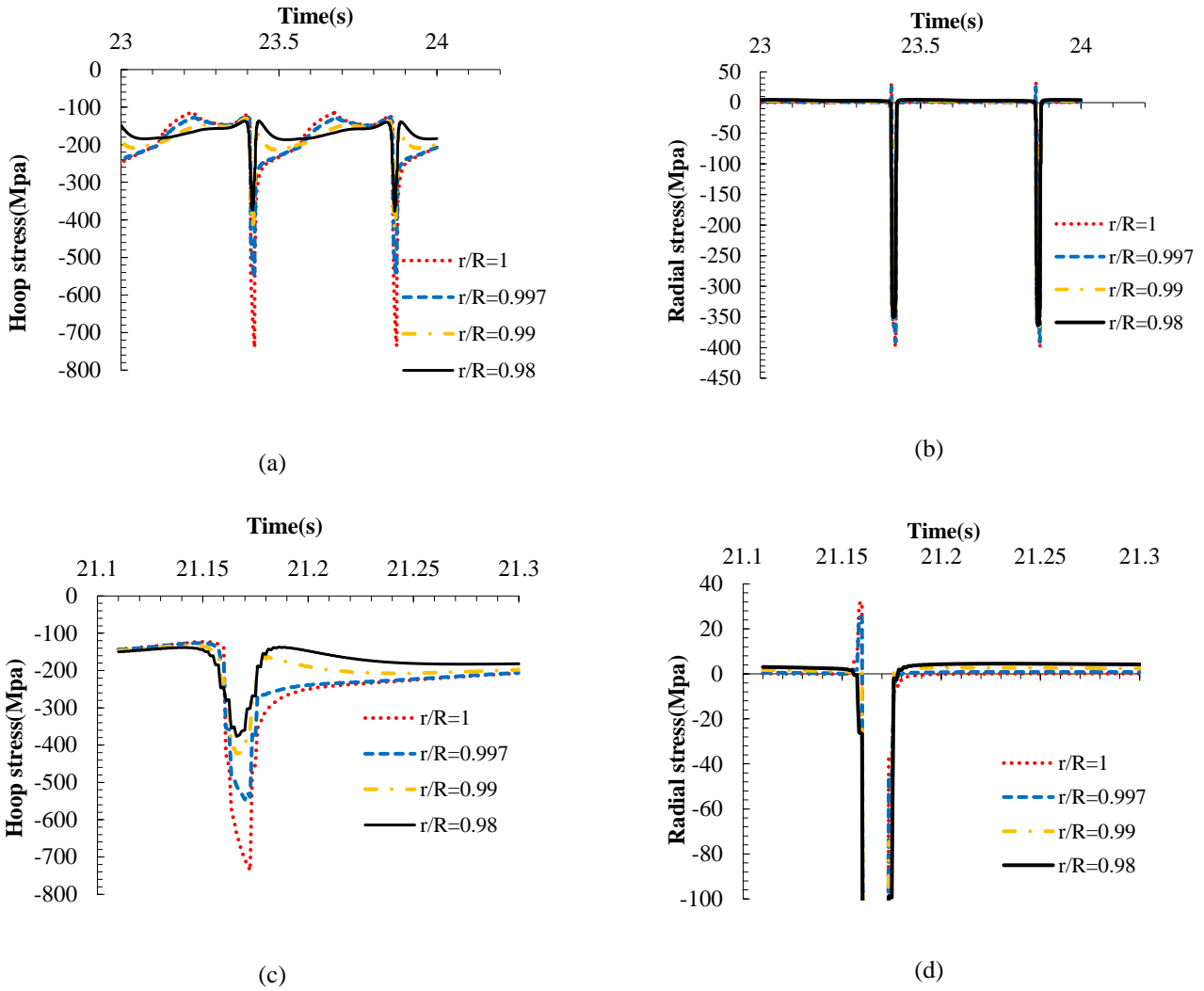


Figure 12: Variation of radial and hoop thermo-mechanical stresses in the mandrel with imposing load (a,b) - detailed view(c,d)

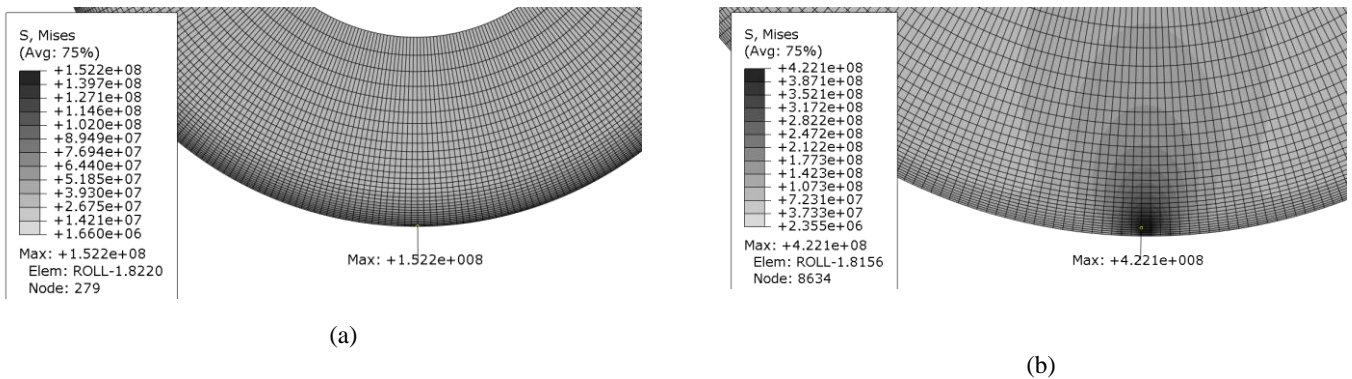


Figure 13: Von-Mises stress of the main roll in 20th seconds of simulation. (a): Thermal stress (b): Thermo-mechanical stress

Figure-12 shows thermo-mechanical stress in the mandrel. Figure 12-a indicates the stress along θ -direction at the end of rolling. In the contact region, the hoop stress reaches -740MPa. Figure 12-c shows the detailed view of the hoop stress. This figure shows that the mandrel surface has the higher stress in the contact region, But in the cooling zone, this value becomes lower than the beneath surface. In both work rolls, this phenomenon occurs in the effective thermal layer. Figures 12-b and 12-d show the stress along r-direction within the specific time period. The magnitudes of radial stress in contact region reaches -400MPa.

Figure 12-d depict the detailed view of figure 12-b in the contact region. The trend of the radial stress is approximately the same as the main roll. It indicates that the magnitude of the radial stress becomes tension before the contact zone. In this region, the magnitude of radial stress reaches 32MPa.

With respect to the thermo-mechanical hoop stresses in figures 11 and 12, it is evident that in the contact region, the compressive stress in the main roll is higher than the mandrel. This is due to smaller contact area in the main roll. However, in the mandrel, the variation of the hoop stress in the effective thermal layer is considerable. For an example, before cooling

zone, the thermo-mechanical stresses in the surface of the main roll and mandrel reaches -77MPa and -207MPa , respectively. It should be underlined that in the thermal layer except for contact area, the thermal stress is the major section of the thermo-mechanical stress. So, it is obvious that in the mandrel the effect of thermal stress on thermo-mechanical stress is noticeable.

Figure 13 shows the Von-Mises thermal and thermo-mechanical stresses in the main roll. The figure 13-a and 13-b show the zoomed view of the roll in the contact region with imposing thermal and thermo-mechanical loads, respectively. With respect to this figures, it is obvious that the maximum Von-Mises stress in figure 13-a is on roll surface but in figure 13-b the maximum value appears below the roll surface. This phenomenon may be explained by Hertzian stress theory. By applying mechanical loads to the roll, the maximum shear stress appears below the surface and influences the amount of equivalent stress in the roll. So, the crack nucleation may take place in this area. Upcoming work will be focused on the effects of thermo-mechanical stress in estimating life.

6. Conclusions

The defect in work rolls directly affects the forming cost and the final shape of the product. The thermo-mechanical stresses may reduce the roll life. The investigation of the thermo-mechanical stress in work roll with real-conditions is complex. So, most of the researchers desire to simplify the geometry and boundary conditions in order to reduce simulation cost. Two-dimensional analyses of rolling have been done with the acceptable result and high computational cost. However, this kind of modeling which uses slightly simplified boundary

conditions on the work rolls is still complicated. It should be emphasized that the study of the ring rolling is more complicated than flat rolling due to the variable rolling force, contact surface, heat flux, and etc. In this research, an integrated finite element model introduced to study the thermo-mechanical behavior of work rolls during hot ring rolling process. Firstly, different modeling methods in ABAQUS were investigated. It is specified that the prepared subroutines in ABAQUS only used in thermal analyses. The proposed attached parts method is not suitable for thermo-mechanical analysis. The virtual thermal properties of attached parts affect the stability limit of simulation. These properties cause very small time increment in the simulation. The developing script codes have an acceptable result and low computational cost. The code is able to use in any geometry and partial boundary conditions. It should be indicated that the variation of the boundary conditions, such as contact surface, heat flux and etc. is carried out during the ring rolling process. The main conclusions are expressed as follow:

1. The results show that all simulation methods give the same trend in temperature field and the most difference has been seen in peak points where the work rolls reach to the ring's contact region.
2. Comparing to the published paper, the implicit algorithm presents the best result in the heating zone in conjunction with acceptable computational time.
3. The proposed developing code reduces computational time; in addition, it is capable to analyze thermo-mechanical simulation simultaneously.
4. The results of simulation show the equations proposed by Tseng et al. is the upper bound for the effective thermal

layer in which variation of temperature and stress are noticeable.

5. Thermal and thermo-mechanical stresses have the different results in the contact zone. However, they expressed the same results in other regions which are consistent with the physics of the problem.
6. The magnitude of hoop and radial stresses are compressive in most of the locations. In the short period of time, the magnitude of radial stress becomes tension before the contact zone.
7. The effect of the thermal stress in the mandrel is noticeable than the main roll. This is due to the thicker effective thermal layer in the mandrel.
8. The effect of mechanical loads in the equivalent stresses should be considered because the magnitude of the thermal and thermo-mechanical stresses is completely different. Thus, it is better to use the thermo-mechanical results for estimating roll life.

References

- [1] T. M.-W. Dortmund, Precision forgings produced on axial closed die rolling lines, *FIA's Forge Fair*, Vol. 88, 1988.
- [2] J. Hawkyard, W. Johnson, J. Kirkland, E. Appleton, Analyses for roll force and torque in ring rolling, with some supporting experiments, *International Journal of Mechanical Sciences*, Vol. 15, No. 11, pp. 873-893, 1973.
- [3] A. Mamalis, W. Johnson, J. Hawkyard, Pressure distribution, roll force and torque in cold ring rolling, *Journal of Mechanical Engineering Science*, Vol. 18, No. 4, pp. 196-209, 1976.
- [4] D. Yang, J. Ryoo, J. Choi, W. Johnson, Analysis of roll torque in profile ring-rolling of L-sections, in *Proceeding of*, Springer, pp. 69-74.
- [5] J. Ryoo, D. Yang, W. Johnson, Lower upper-bound analysis of the ring rolling process by using force polygon diagram and dual velocity field, *Advanced Technology Plasticity*, Vol. 2, pp. 1292-1298, 1984.
- [6] P. Stevens, K. Ivens, P. Harper, Increasing work-roll life by improved roll-cooling practice, *J Iron Steel Inst*, Vol. 209, No. 1, pp. 1-11, 1971.
- [7] A. Tseng, S. Tong, F. Lin, Thermal stresses of rotating rolls in rolling processing, *Journal of Thermal Stresses*, Vol. 12, No. 4, pp. 427-450, 1989.
- [8] E. Patula, Steady-state temperature distribution in a rotating roll subject to surface heat fluxes and convective cooling, *ASME Journal of heat transfer*, Vol. 103, No. 1, pp. 36-41, 1981.
- [9] W. Yuen, On the steady-state temperature distribution in a rotating cylinder subject to heating and cooling over its surface, *ASME Journal of Heat Transfer*, Vol. 106, No. 3, pp. 578-585, 1984.
- [10] A. C. Yiannopoulos, N. Anifantis, A. Dimarogonas, Thermal stress optimization in metal rolling, *Journal of thermal stresses*, Vol. 20, No. 6, pp. 569-590, 1997.
- [11] A. Afshin, M. Zamani Nejad, K. Dastani, Transient thermoelastic analysis of FGM rotating thick cylindrical pressure vessels under arbitrary boundary and initial conditions, *Journal of Computational Applied Mechanics*, Vol. 48, No. 1, pp. 15-26, 2017.
- [12] M. Gharibi, M. Z. Nejad, A. Hadi, Elastic analysis of functionally graded rotating thick cylindrical pressure vessels with exponentially-varying properties using power series method of Frobenius, *Journal of Computational Applied Mechanics*, Vol. 48, No. 1, pp. 89-98, 2017.

- [13] N. Razani, B. M. Dariani, M. Soltanpour, Analytical approach of asymmetrical thermomechanical rolling by slab method, *The International Journal of Advanced Manufacturing Technology*, Vol. 94, No. 1-4, pp. 175-189, 2018.
- [14] O. Zienkiewicz, E. Oñae, J. Heinrich, A general formulation for coupled thermal flow of metals using finite elements, *International Journal for Numerical Methods in Engineering*, Vol. 17, No. 10, pp. 1497-1514, 1981.
- [15] A. Tseng, A numerical heat transfer analysis of strip rolling, *Journal of heat transfer*, Vol. 106, No. 3, pp. 512-517, 1984.
- [16] P. Gratacos, P. Montmitonnet, C. Fromholz, J. Chenot, A plane-strain elastoplastic finite-element model for cold rolling of thin strip, *International journal of mechanical sciences*, Vol. 34, No. 3, pp. 195-210, 1992.
- [17] W. Lai, T. Chen, C. Weng, Transient thermal stresses of work roll by coupled thermoelasticity, *Computational mechanics*, Vol. 9, No. 1, pp. 55-71, 1991.
- [18] D.-F. Chang, Thermal stresses in work rolls during the rolling of metal strip, *Journal of materials processing technology*, Vol. 94, No. 1, pp. 45-51, 1999.
- [19] P.-T. Hsu, Y.-T. Yang, A three-dimensional inverse problem of estimating the surface thermal behavior of the working roll in rolling process, *Journal of manufacturing science and engineering*, Vol. 122, No. 1, pp. 76-82, 2000.
- [20] S. Serajzadeh, A. K. Taheri, F. Mucciardi, Unsteady state work-roll temperature distribution during continuous hot slab rolling, *International Journal of Mechanical Sciences*, Vol. 44, No. 12, pp. 2447-2462, 2002.
- [21] F. Fischer, W. Schreiner, E. Werner, C. Sun, The temperature and stress fields developing in rolls during hot rolling, *Journal of materials processing technology*, Vol. 150, No. 3, pp. 263-269, 2004.
- [22] J. Song, A. Dowson, M. Jacobs, J. Brooks, I. Beden, Coupled thermo-mechanical finite-element modelling of hot ring rolling process, *Journal of Materials Processing Technology*, Vol. 121, No. 2, pp. 332-340, 2002.
- [23] D. Benasciutti, E. Brusa, G. Bazzaro, Finite elements prediction of thermal stresses in work roll of hot rolling mills, *Procedia Engineering*, Vol. 2, No. 1, pp. 707-716, 2010.
- [24] D. Benasciutti, On thermal stress and fatigue life evaluation in work rolls of hot rolling mill, *The Journal of Strain Analysis for Engineering Design*, Vol. 47, No. 5, pp. 297-312, 2012.
- [25] A. Draganis, F. Larsson, A. Ekberg, Finite element analysis of transient thermomechanical rolling contact using an efficient arbitrary Lagrangian–Eulerian description, *Computational Mechanics*, Vol. 54, No. 2, pp. 389-405, 2014.
- [26] H. Sayadi, S. Serajzadeh, Prediction of thermal responses in continuous hot strip rolling processes, *Production Engineering*, Vol. 9, No. 1, pp. 79-86, 2015.
- [27] F. Qayyum, M. Shah, S. Manzoor, M. Abbas, Comparison of thermomechanical stresses produced in work rolls during hot and cold rolling of Cartridge Brass 1101, *Materials Science and Technology*, Vol. 31, No. 3, pp. 317-324, 2015.
- [28] A. Milenin, R. Kuziak, M. Lech-Grega, A. Chochorowski, S. Witek, M. Pietrzyk, Numerical modeling and experimental identification of residual stresses in hot-rolled strips, *Archives of civil and mechanical engineering*, Vol. 16, No. 1, pp. 125-134, 2016.
- [29] B. Koohbor, Finite element modeling of thermal and mechanical stresses in work-rolls of warm strip rolling process, *Proceedings of the Institution of Mechanical Engineers, Part B: Journal of Engineering Manufacture*, Vol. 230, No. 6, pp. 1076-1086, 2016.
- [30] D. Benasciutti, F. De Bona, M. G. Munteanu, A harmonic one-dimensional element for non-linear thermo-mechanical analysis of axisymmetric structures under asymmetric loads: The case of hot strip rolling, *The Journal of Strain Analysis for Engineering Design*, Vol. 51, No. 7, pp. 518-531, 2016.
- [31] G. Deng, Q. Zhu, K. Tieu, H. Zhu, M. Reid, A. A. Saleh, L. Su, T. D. Ta, J. Zhang, C. Lu, Evolution of microstructure, temperature and stress in a high speed steel work roll during hot rolling: Experiment and modelling, *Journal of Materials Processing Technology*, Vol. 240, pp. 200-208, 2017.
- [32] K. H. Huebner, D. L. Dewhirst, D. E. Smith, T. G. Byrom, 2008, *The finite element method for engineers*, John Wiley & Sons,
- [33] M. Balla, Formulation of coupled problems of thermo-elasticity by finite elements, *Periodica Polytechnica. Engineering. Mechanical Engineering*, Vol. 33, No. 1-2, pp. 59, 1989.
- [34] ABAQUS, ABAQUS Documentation, Dassault Systèmes, 2013.
- [35] A. Negahban, A. Maracy, E. Barati, Investigation of 2-D Hot Ring Rolling Simulation and Effects of Different Parameters on Forming Process of Jet's Spool, *Journal of aeronautical engineering*, Vol. 18, No. 1, pp. 75-92, 2016. "(in Persian)"
- [36] L. Hua, X. Huang, C. Zhu, Theory and technology of ring rolling, *China Mechanical Industry Press, Beijing*, 2001.
- [37] J. Benedyk, Aerospace And High Performance Alloys Database, *UNE*, Vol. 36072, No. 2.
- [38] eFunda, www.efunda.com, Accessed.
- [39] H. Yan, G. Qian, Q. Hu, Development of flow stress of AISI H13 die steel in hard machining, *Journal of Wuhan University of Technology-Mater. Sci. Ed.*, Vol. 22, No. 2, pp. 187-190, 2007.
- [40] M. Forouzan, M. Salimi, M. Gadala, Three-dimensional FE analysis of ring rolling by employing thermal spokes method, *International journal of mechanical sciences*, Vol. 45, No. 12, pp. 1975-1998, 2003.
- [41] A. Tseng, S. Tong, S. Maslen, J. Mills, Thermal behavior of aluminum rolling, *Journal of Heat Transfer*, Vol. 112, No. 2, pp. 301-308, 1990.
- [42] A. Tseng, F. Lin, A. Gunderia, D. Ni, Roll cooling and its relationship to roll life, *Metallurgical Transactions A*, Vol. 20, No. 11, pp. 2305, 1989.
- [43] R. D. Cook, 1994, *Finite element modeling for stress analysis*, Wiley,
- [44] A. Sonboli, S. Serajzadeh, A model for evaluating thermo-mechanical stresses within work-rolls in hot-strip rolling, *Journal of Engineering Mathematics*, Vol. 72, No. 1, pp. 73-85, 2012.